Archives of Materials Science and Engineering

Volume 28
Issue 9
September 2007
Pages 549-556

International Scientific Journal
published monthly as the organ of
the Committee of Materials Science
of the Polish Academy of Sciences

Mechanical properties of monolayer coatings deposited by PVD techniques

L.A. Dobrzański *, K. Lukaszkowicz
Division of Materials Processing Technology, Management and Computer Techniques in Materials Science, Institute of Engineering Materials and Biomaterials, Silesian University of Technology, ul. Konarskiego 18a, 44-100 Gliwice, Poland
* Corresponding author: E-mail address: leszek.dobrzanski@polsl.pl

Received 01.06.2007; published in revised form 01.09.2007

ABSTRACT

Purpose: This research was done to investigate the mechanical properties of monolayer coatings (Ti/CrN, Ti/TiAlN, Ti/ZrN, CrN, TiAl/TiAlN, Zr/ZrN, TiN) deposited by PVD technique (reactive magnetron sputtering method) onto the substrate from the CuZn40Pb2 brass. A thin metallic layer was deposited prior to deposition of ceramic monolithic coatings to improve adhesion.

Design/methodology/approach: The microstructure of the coatings was cross section examined using scanning electron microscope. The residual stress was obtained from the parabolic deflection of the samples, after the coating deposition applying Stoney's equation. The microhardness and Young's modulus tests were made on the dynamic ultra-microhardness tester. Tests of the coatings' adhesion to the substrate material were made using the scratch test.

Findings: Obtained results show that all the coatings are in a state of compressive residual stress. The stiffness of the examined coatings is between 224-330 mN/μm, while Young's modulus is between 258-348 GPa. Concerning the adhesion of the coatings measured by scratch test, it has been stated that the critical load L_{C2} for coatings, deposited onto the brass ranges from 41 to 57 N.

Research limitations/implications: In order to evaluate with more detail the possibility of applying these coatings in tools, further investigations should be concentrated on the determination of the tribological properties of the coatings.

Originality/value: The paper contributes to better understanding and recognition the structure of thin coatings deposited by PVD techniques. It should be stressed that the mechanical properties of the PVD coatings obtained in this work are very encouraging and therefore their application for products manufactured at mass scale is possible in all cases where reliable, very hard and abrasion resistant coatings, deposited onto brass substrate are needed.

Keywords: Thin&thick Coatings; Residual stresses; Scratch test; Young's modulus, Microhardness

PROPERTIES

1. Introduction

Deposition of hard layers of nitrides, carbides or oxides on material surface in the PVD processes is one of the most intensely developed directions of improvement of working properties of functional elements. Hard coatings with metal nitrides, like CrN, TiAlN, TiN, ZrN, etc., extend the life of the items that were covered with them, improving not only their wear resistance but also their resistance to the chemically aggressive environment, in comparison to the non-coated metal materials. However, wear resistance of coatings depends on many other factors, including hardness, elastic modulus, friction, fracture toughness [1-4].

Adhesion of the coating to the substrate features one of the key issues pertaining to coating items with the hard ceramic materials. Therefore, the coating-substrate contact zone is important when the reliable and durable coating is to be worked out [5-7]. Employment of the thin interlayer, e.g., Ti or Cr results in improvement of the proper coating adhesion, as the soft

titanium or chromium layer reduces stresses and counteracts propagation of cracks [8-10].

Thin, hard PVD coatings on a soft base, e.g. brass, turn out to be an advantageous material combination from the tribological point of view. They increase their resistance to scratches and crevices developing in contact with hard materials. They have the particular role for protection from wear or corrosive wear. One of the limitations in using hard coatings on a relatively soft base is developing of high stresses in coatings and in the substrate material – coating contact zone, when the coating is loaded and the material is being bent [11-13].

Internal stresses feature a serious problem connected with thin coatings deposited by PVD processes. Mechanical properties, like hardness, adhesion, and tribological properties of the applied coatings are strongly contingent upon the values and spatial distribution of the internal stresses. All residual stresses values indicate to the compression (negative) residual stresses in the deposited coatings. The internal (micro-structural) stresses prevail in this case. The external (thermal) stresses are predominant in the chemical vapour deposition processes (CVD), as these processes are carried out at higher temperature. The compression stresses in coatings improve their mechanical properties. One can notice that residual stresses in coatings grow along with the increase of the accelerating potential. However, the excessive compression stresses may induce problems with good adhesion of coatings to their substrate, close to the edge in particular, which is demonstrated by delamination or spalling of coating from the substrate [14-20].

The goal of this work is investigation of the mechanical properties of the monolayer coatings deposited by magnetron sputtering onto the brass substrate.

2. Investigation methodology

The coatings were produced by reactive dc magnetron sputtering using metallic pure targets. They were deposited on CuZn40Pb2 brass substrates. One of the thin interlayer from the pure Cr, Ti, Zr, or the TiAl alloy (about 100 nm) were applied onto the substrate to improve the coatings' adhesion. Some deposition conditions are summarized in table 1.

The structures of the deposited coatings were examined on transverse sections in a Philips XL-30 scanning electron microscope. Secondary electrons were used for generation of fracture images. The accelerating voltage was 20 kV.

The thickness of coatings was determined using the "kalotest" method, consisting in measuring the characteristic features of the crater developed in the coated specimen's surface. The coating thickness was determined by using the following relationship relevant to this setup:

$$g = \frac{D^2 - d^2}{8 \cdot R} \cdot 10^3 \tag{1}$$

where:
g – coating thickness [μm];
d – crater inner diameter [mm];
D – crater outer diameter [mm];
R – ball diameter [mm].

Techniques used for measurements of the residual stresses are based on the deflection the thin specimens after the coating deposition process. The dimensions of the brass substrates for residual stress measurements were: diameter of 25 mm and thickness of 500 μm. The curvature radius of the coated and uncoated specimens was measured by laser triangulation over the specimen surface in two perpendicular directions (Fig. 1). The residual stresses σ_{res} were calculated using the Stoney's equation [14, 21]:

$$\sigma_{res} = -\frac{E_s \cdot t_s^2}{6 \cdot t_c \cdot (1 - \upsilon_s)} \left(\frac{1}{r_a} - \frac{1}{r_b} \right) \tag{2}$$

where:
E_s, t_s and υ_s – Young`s modulus, thickness, and Poisson ratio of the substrate (respectively);
t_c – coating thickness;
r_a and r_b – the specimen surface curvature radii before and after the deposition of the coating.

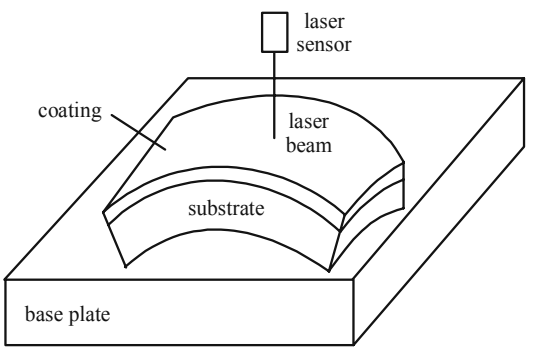

Fig. 1. The schema of the laser triangulation apparatus to measure the curvature radius of the specimens in order to determine the residual stresses.

The microhardness tests were made on the SHIMADZU DUH 202 dynamic ultra-microhardness tester. The tests were made under the load 25 mN, enabling the operator to minimize the influence of the substrate on the obtained results, so that the indentation depth was lower than 1/10 of the thickness of the deposited coatings.

The Young's modulus was calculated using the Hardness 4.2 software package delivered as a part of the ultra-microhardness tester system, according to the formula:

$$\frac{1}{E_r} = \frac{1 - \upsilon_i^2}{E_i} + \frac{1 - \upsilon_s^2}{E_s} \tag{3}$$

where:
E_r – reduced Young`s modulus [kN/mm^2];
E_s, E_i – Young`s moduli of the substrate and indenter (respectively) [kN/mm^2];
υ_s, υ_i – Poisson ratio of the substrate and indenter (respectively).

Table 1.
Coating types and their deposition parameter: *during metallic layers deposition; ** during ceramic layers deposition

Coating type	Numbers of layers	Substrate bias voltage, V	Chamber pressure, Pa	Partial pressure, Pa		Temperature, ^{o}C
				nitrogen	argon	
Ti/CrN	1	-50	0.58	0* 0.15**	0.31	300
Ti/ZrN	1	-50	0.34	0* 0.10**	0.29	
Ti/TiAlN	1	-40	0.40	0* 0.10**	0.38	
Cr/CrN	1	-50	0.39	0* 0.15**	0.30	
Ti/TiN	1	-60	0.25	0* 0.07**	0.25	
Zr/ZrN	1	-60	0.35	0* 0.10**	0.29	
TiAl/TiAlN	1	-60	0.49	0* 0.11**	0.45	

Tests of the coatings' adhesion to the substrate material were made using the scratch test, routinely employed in case of the coatings obtained in processes of physical vapour deposition. In this method, the diamond indenter with the Rockwell C type tip travels on the examined specimen's surface at a constant speed with the continuously increasing load force. The tests were made on the computer controlled Sebastian 5A (Quad Group) device equipped with the acoustic detector, at the following conditions:

- load increase rate (dL/dt) – 100 N/min;
- indenter feed rate (dx/dt) – 10 mm/min.

3. Discussion of results

The structure of the coatings was examined on the transverse surfaces of fractures in the electron scanning microscope. The coatings display equal thickness over their entire area. The columnar structure of the monolayer coatings is clearly visible (Fig. 2).

The values of the critical load L_{C2} characterized by adhesion of the examined coatings to the CuZn40PB2 brass substrate, caused mainly by the forces of adhesion, have been determined using the scratch test with a linear growing load (Fig. 3-9).

The second critical load L_{C2} is the point at which the damage becomes continuous and complete delamination of the coating start; the first appearance of cracking chipping, spallation and delamination outside or inside the track with the exposure of the material substrate – the first adhesion-related failure event. After this point, all of the acoustic emission, friction force signals become noisier [22, 23]. The summary results are presented in Table 2. Employment of the additional thin (Ti, Zr, Cr, TiAl) interlayer in monolayers improves adhesion of the nitride coating to the substrate, as it counteracts propagation of cracks and reduces stresses in the coating-substrate zone.

Examinations of changes of the chemical concentrations of the coating constituents and substrate material carried out on the GDOS glow-discharge optical emission spectroscope are presented in Fig. 10-16.

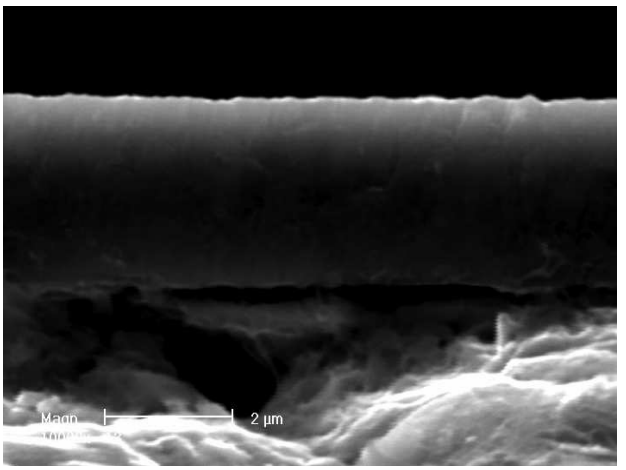

Fig. 2. Fracture of the Zr/ZrN coating deposited onto the substrate from the CuZn40Pb2 brass

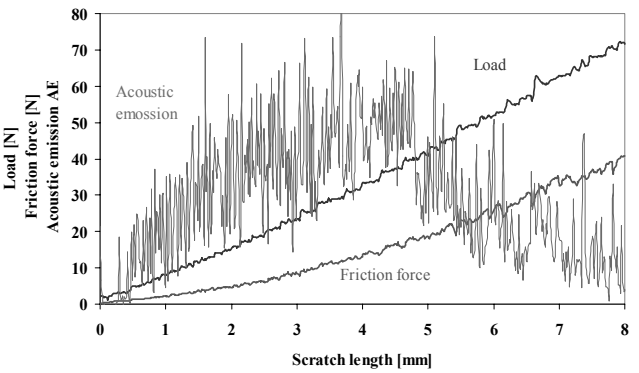

Fig. 3. Plot of the dependence of the acoustic emission and friction force from the scratch path for the Ti/CrN coating deposited onto the CuZn40Pb2 substrate

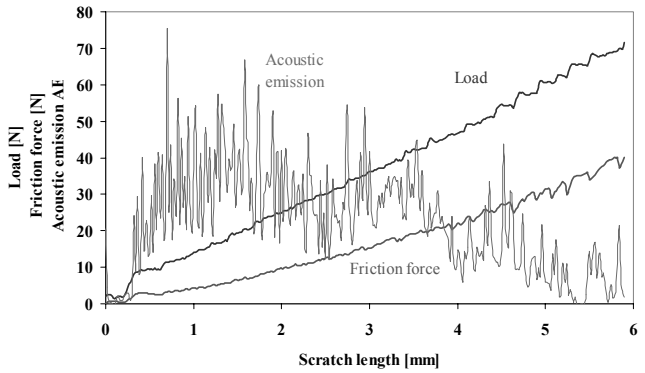

Fig. 4. Plot of the dependence of the acoustic emission and friction force from the scratch path for the Ti/ZrN coating deposited onto the CuZn40Pb2 substrate

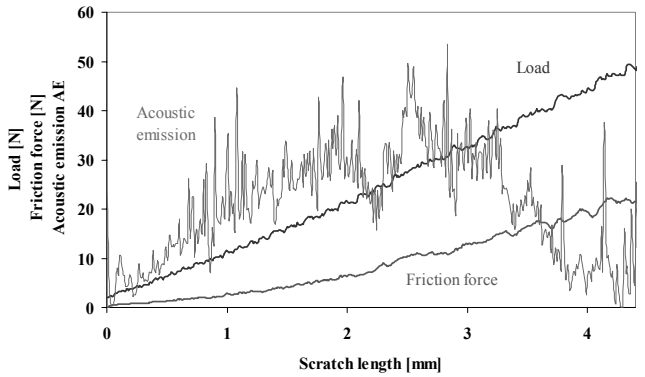

Fig. 5. Plot of the dependence of the acoustic emission and friction force from the scratch path for the Ti/TiAlN coating deposited onto the CuZn40Pb2 substrate

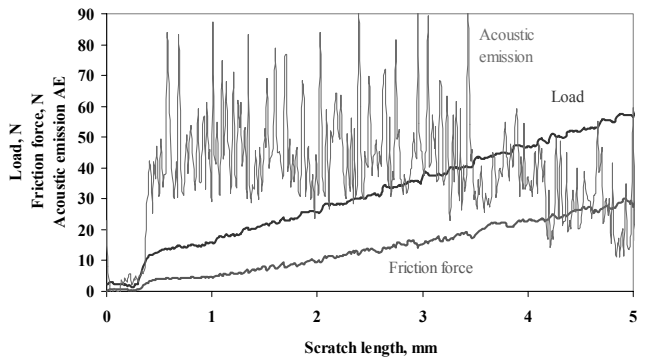

Fig. 6. Plot of the dependence of the acoustic emission and friction force from the scratch path for the Cr/CrN coating deposited onto the CuZn40Pb2 substrate

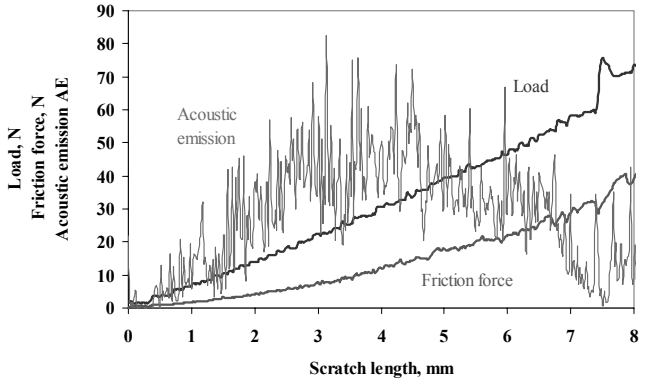

Fig. 7. Plot of the dependence of the acoustic emission and friction force from the scratch path for the Ti/TiN coating deposited onto the CuZn40Pb2 substrate

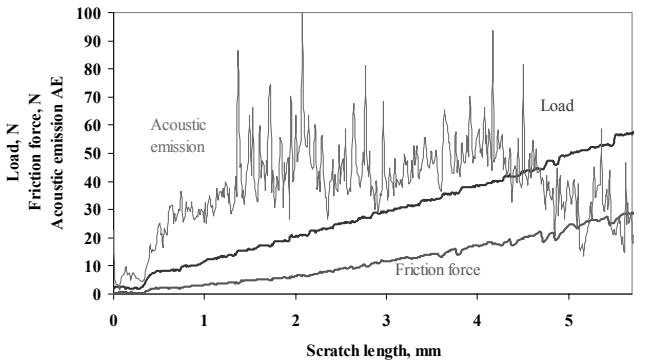

Fig. 8. Plot of the dependence of the acoustic emission and friction force from the scratch path for the Zr/ZrN coating deposited onto the CuZn40Pb2 substrate

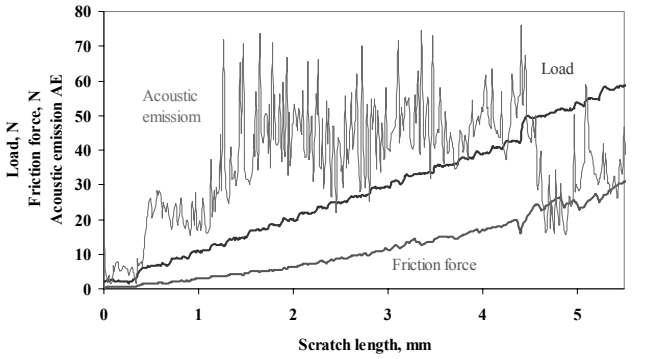

Fig. 9. Plot of the dependence of the acoustic emission and friction force from the scratch path for the TiAl/TiAlN coating deposited onto the CuZn40Pb2 substrate

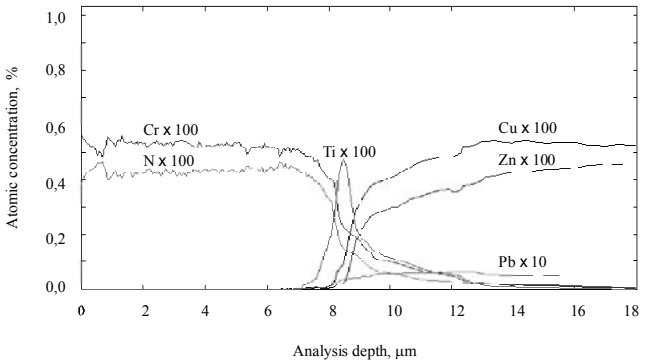

Fig. 10. Changes of concentrations of constituents of the Ti/CrN coating and of the substrate material

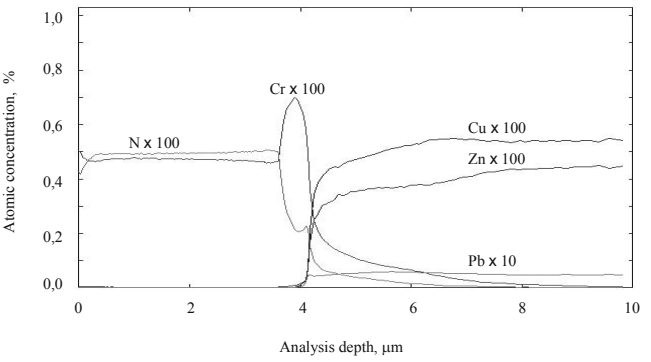

Fig. 13. Changes of concentrations of constituents of the Cr/CrN and of the substrate material

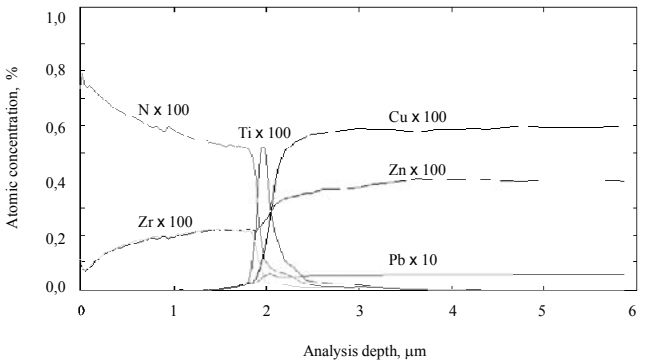

Fig. 11. Changes of concentrations of constituents of the Ti/ZrN coating and of the substrate material

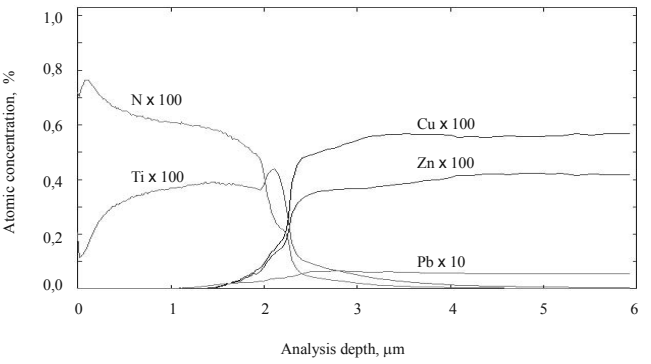

Fig. 14. Changes of concentrations of constituents of the Ti/TiN and of the substrate material

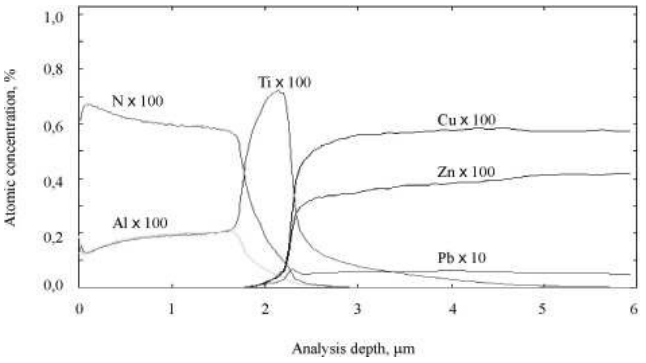

Fig. 12. Changes of concentrations of constituents of the Ti/TiAlN coating and of the substrate material

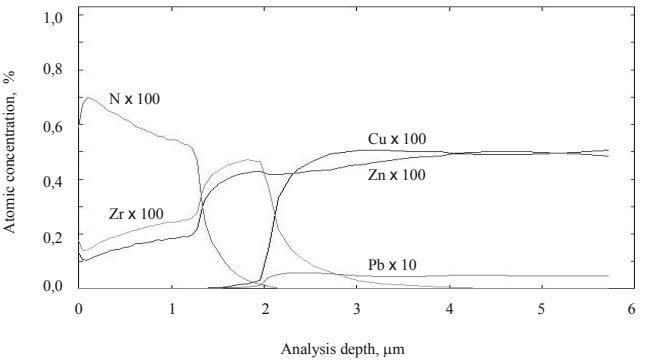

Fig. 15. Changes of concentrations of constituents of the Zr/ZrN and of the substrate material

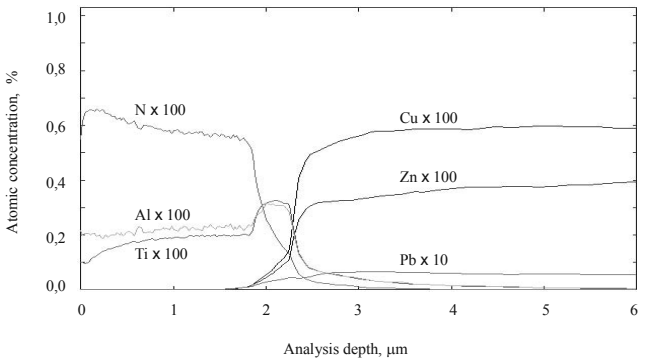

Fig. 16. Changes of concentrations of constituents of the TiAl/TiAlN and of the substrate material

Varying concentrations of elements constituting the Ti/CrN coatings (Fig. 10) attests its chemical inhomogeneity. The chemical composition of the Ti/ZrN coatings also differs from the equilibrium one (Fig. 11). The nitrogen concentration decreases steadily, whereas the Zr concentration grows. A similar situation occurs in case of the Ti/TiAlN coatings (Fig. 12), where also concentration changes of the pure Ti and Al metals forming the coating, and also nitrogen are significant. In the Cr/CrN coating (Fig. 13) their chemical composition is close to the equilibrium one. However, for Zr/ZrN, Ti/TiN, TiAl/TiAlN coatings (Fig. 14-16) differences occur in concentrations of the particular elements, which may be caused by origination of the solid secondary solutions or by the inhomogeneous evaporation of the material from the specimen surface during examinations in the spectrometer. However, basing on the analysis of the chemical composition from the micro-areas of coatings it was found out that it is close to the equilibrium one. In case of monolyaers one can easily notice the thin interlayers, whose goal is to increase adhesion of the proper coating to the substrate.

The investigations made using the glow discharge optical emission spectrometer GDOS indicate that in the analysed cases, in the joint zone, concentration of elements included in the substrate grows with the simultaneous rapidly decreasing concentration of elements constituting the coatings. This may attest to the existence of the interface between the substrate material and the coating, resulting in improvement of adherence between the deposited coatings to the substrate, albeit these results cannot be interpreted unequivocally because of the inhomogeneous vaporizing of the material from the specimens' surfaces. The existence of the interface should be also connected with the increase of desorption of the substrate surface and development of defects in the substrate as well as with displacement of elements in the joint zone due to interaction of the high-energy ions. In spite of the indicated interpretation ambiguities, the obtained results are close to those published in [24, 25].

The obtained results show that the coatings are under compressive (negative) residual stress (Table 2). In this case the dominant role is played by the internal stresses, connected to the growing process itself. The external (thermal) stresses are not significant because the deposition temperatures are relatively low. The compressive stresses in the coatings, within certain limits, cause the increase of their endurance properties and especially hardness. Too big compressive stresses may, however, cause adhesion problems, as in case of Ti/TiAl and Ti/ZrN coating (Table 2), especially close to the edge.

Hardness tests of the deposited coatings were made in the 'load-unload' mode, in which loading of the indenter with a specified force takes place, holding it for the predetermined time, and then the indenter load force is released (Fig. 17, 18). When carrying out the test, one can observe not only plastic deformation of the material but also its elastic deformation. Microhardness determined this way is called dynamical microhardness. The precise meter circuit allows registering the depth of the created imprint while loading or unloading the indenter. The summary results are presented in Table 2.

With the use of the Hardness 4.2 software package, which is part of the ultramicrohardness tester, and the dependency between the load and the depth of the indenter into the examined coating (Fig. 17,18), the Young's modulus as well as the stiffness of coatings, have been determined (Table 2). The stiffness of the examined coatings is between 224-330 mN/μm, whereas Young's modulus is between 258-348 GPa.

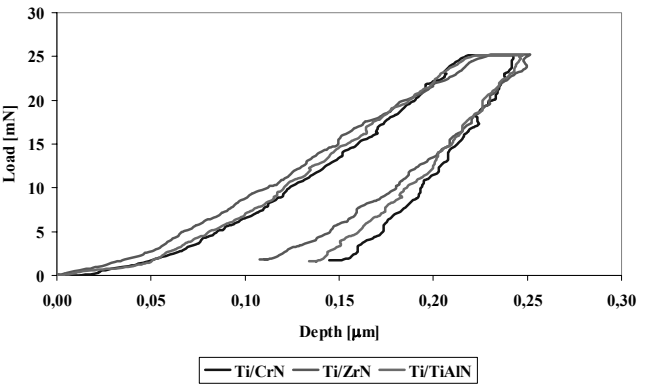

Fig. 17. Plot of the load/unload curves as a function of the depth for Ti/CrN, Ti/ZrN and Ti/TiAlN coatings

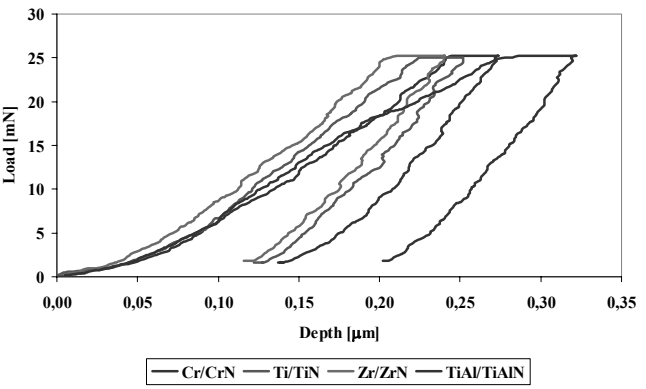

Fig. 18. Plot of the load/unload curves as a function of the depth for Cr/CrN, Ti/TiN, Zr/ZrN and Ti/TiAlN coatings

Table 2.
Summary results of the mechanical properties

Coating type	Residual stresses, GPa	Critical load L_{C2}, N	Hardness DHV0,0025	Young`s modulus, GPa	Stiffness, mN/μm	Thickness, μm
Ti/CrN	-2.6	50	2450	258	330	5.8
Ti/ZrN	-8.9	45	3100	291	224	2.1
Ti/TiAlN	-11.9	41	2400	348	274	2.3
Cr/CrN	-10.5	48	2400	274	255	3.6
Ti/TiN	-4.2	57	2800	293	228	2.4
Zr/ZrN	-5.6	48	3100	345	252	2.0
TiAl/TiAlN	-0.3	50	2200	277	239	2.3

4. Conclusions

The investigations made using the glow discharge optical emission spectrometer GDOS indicate to the existence of the interface between the substrate material and the coating resulting in improvement of the adhesion of the coatings deposited to the substrate.

Good adhesion of the coatings deposited to the substrate should be connected with the existence of the interface and interlayer from the pure metal. This may be attested by the critical load L_{C2}, which is in the range 57-41 N, depending on the coating type.

Mechanism of the PVD coatings failure revealed by the adhesion test is connected with the arc shaped cracks caused by tension and spalling occurring at the bottom of the developing scratch.

In the investigated coatings the negative (compression) internal stresses occur, causing improvement of their tribological and mechanical properties, including their adhesion to the substrate.

The stiffness of the examined coatings is between 224-330 mN/μm, while Young's modulus is between 258-348 GPa.

Acknowledgements

Authors would like to express their thanks to the associates of Physics Department at the School of Science, University of Minho in Portugal for their assistance in carrying out the research.

References

[1] L.A. Dobrzański, K. Lukaszkowicz, D. Pakuła, J. Mikuła, Corrosion resistance of multilayer and gradient coatings deposited by PVD and CVD techniques, Archives of Materials Science and Engineering 28 (2007) 12-18.

[2] A. Erdemir, Review of engineering tribological interfaces for improved boundary lubrication, Tribology International 38 (2005) 249-256.

[3] M. Andritschky, Protective coatings on high temperature steel applied by PVD deposition techniques, Journal of Materials Processing Technology 53 (1995) 33-46.

[4] P.H. Mayrhofer, C. Mitterer, L. Hultman, H. Clemens, Microstructural design of hard coatings, Progress in Materials Science 51 (2006) 1032-1114.

[5] D.N. Allsopp, I. M. Hutchings, Micro-scale abrasion and scratch response of PVD coatings at elevated temperature, Wear 251 (2001) 1308-1314.

[6] R. Hoy, J.D. Kamminga, G.C.A.M. Janssen, Scratch resistance of CrN coatings on nitrided steel, Surface and Coatings Technology 200 (2006) 3856-3860.

[7] R. Jacobs, J. Meneve, G. Dyson, D.G. Teer, N.M. Jennett, P. Harris, J. von Stebut, C. Comte, P. Feuchter, A. Cavaleiro, H.Ronkainen, K. Holmberg, U. Beck, G. Reiners, C.D. Ingelbrecht, A certified material for the scratch test, Surface and Coatings Technology 174-175 (2003) 1008-1013.

[8] L. A. Dobrzański, K. Lukaszkowicz, Erosion resistance and tribological properties of coatings deposited by reactive magnetron sputtering method onto the brass substrate, Journal of Materials Processing Technology 157-158 (2004) 317-323.

[9] F. Ashrafizadeh, Adhesion evaluated of PVD coatings to aluminium substrate, Surface and Coatings Technology 130 (2000) 186-194.

[10] B. Navinsek, P. Panjan, M. Cekada, D.T. Quinto, Interface characterization of combination hard/solid lubricant coatings by specific methods, Surface and Coatings Technology 154 (2002) 194-203.

[11] K. Holmberg, A. Matthews, Coating Tribology, Elsevier, Amsterdam, 1994.

[12] K. Lukaszkowicz, L.A. Dobrzański, A. Zarychta, L. Cunha: Mechanical properties of multilayer coatings deposited by PVD techniques onto the brass substrate, Journal of Achievements in Materials and Manufacturing Engineering 15 (2006) 47-52.

[13] M. Koch, Use of ion beam etching for producing topographical microstructure, Practical Metallography 36 (1999) 233-249.

[14] J. Y. Robic, H. Leplan, Y. Pauleau, B. Rafin, REsidual stress in silicon dioxide thin films produced by ion-assisted deposition, Thin Solid Films 290-291 (1996) 34-39.

[15] V. Teixeira, Residual stress and cracking in thin PVD coatings, Vacuum 64 (2002) 393-399.

[16] X.L. Peng, Y. Tsui, T. Clyne, Stiffness, residual stresses and interfacial fracture energy of diamond films on titanium, Diamond and Related Materials 6 (1997) 1612-1621.

[17] A.C. Vlasveld, S.G. Harris, E.D. Doyle, D.B. Lewis, W.D. Munz, Characterisation and performance of partially filtered arc TiAlN coatings, Surface and Coatings Technology 149 (2002) 217-224.

[18] L.A. Dobrzański, K. Lukaszkowicz, A. Zarychta, Mechanical properties of monolayer coatings deposited by PVD techniques, Journal of Achievements in Materials and Manufacturing Engineering 20 (2007) 423-426.
[19] C. Johnson, J. Ruud, R. Bruce, D. Wortman, Relationships between residual stress, microstructure and mechanical properties of electron beam-physical vapor deposition thermal barrier coatings, Surface and Coatings Technology 108/109 (1998) 80-85.
[20] W. Weng-Jin, H. Min-Hsiung, The effect of residual stress on adhesion of silicon-containing diamond-like carbon coatings, Thin Solid Films 345 (1999) 200-207.
[21] M. Larson, P. Hedenqvist, S. Hogmark, Deflection measurements as method to determine residual stress in thin hard coatings on tool materials, Surface Engineering 12 (1996) 43-48.
[22] A.O. Sergici, N.X. Randall, Scratch testing of coatings, Advanced Materials and Processes 4 (2006) 1-3.
[23] Y. He, I. Apachitei, J. Zhou, T. Walstock, J. Duszczyk, Effect of prior plasma nitriding applied to a hot-work tool steel on the scratch-resistant properties of PACVD TiBN and TiCN coatings, Surface and Coatings Technology 201 (2006) 2534-2539.
[24] J. Musil, H. Hruby, Superhard nanocomposite $Ti_{1-x}Al_xN$ films prepared by magnetron sputtering, Thin Solid Films 365 (2000) 104-109.
[25] Z. Weiss, K. Marshall, Elemental depth profiling of coated and surface-modified materials by GD-OES: hard coatings on cutting tools, Thin Solid Films 308-309 (1997) 382-388.